Journal of Engineering and Development, Vol. 11, No. 1, March (2007) **ISSN 1813-7822**

The Prediction of Environment Effect on the Performance of a Vapor Compression Refrigeration System in Air Conditioning Application

Dr. Ali Hussain Tarrad
Mechanical Engineering Dept., College of Eng.
Al-Mustansiriya University, Baghdad, Iraq

Asst. Lect. Usama Sami Shehhab
Mechanical Engineering Dept., College of Eng.
Al-Mosul University, Mosul, Iraq

Abstract

This investigation deals with the performance prediction of air conditioning unit. Theoretical and experimental studies were conducted to simulate the performance of vapor compression refrigeration cycle, using R-22 as a circulating refrigerant. The experimental work was carried out on an available air cooling unit which allows variation of different parameters such as air dry bulb temperature, flow rate and humidity affecting the operation conditions of the unit. The comparison between the predicted and experimental data of (COP), cooling load, compressor work and condenser load showed a very good agreement.

Also a detailed design of finned tube evaporator heat exchanger coil in air conditioning unit was developed. Here, the vaporization and superheating portions of heat exchanger have been modeled separately to predict the exit air condition, dry bulb temperature and humidity content, at the leaving section of the cooling coil. The evaporator mathematical model showed a well agreement with the experimental data of this research.

الخلاصـــــة

يتعامل هذا البحث مع التنبؤ بأداء منظومة تكييف ألهواء. لقد تم إجراء دراسة نظرية و عملية لمحاكاة أداء منظومة تبريد إنضغاطية باستخدام (فريون -٢٢) كمائع مدور عبر المنظومة. تم تنفيذ الجانب العملي للبحث باستخدام وحدة تبريد هواء متوفرة والتي تسمح بتغيير عدة متغيرات للهواء مثل درجة حرارة البصلة الجافة، معدل التدفق و الرطوبة والتي تؤثر على الشروط التشغيلية للوحدة. لقد بينت المقارنة بين القيم العملية و النظرية تطابق جيد لمعامل الأداء، حمل التبريد، شغل الضاغط وحمل المكثف.

كذلك تم بناء طريقة تصميم تفصيلية للمبخرات ذات الأنابيب المزعنفة والمستخدمة في منظومات تبريد الهواء. وهنا تم نمذجة المبخر بمنطقتين منفصلتين و المعروفة بمنطقتي التبخير و التحميص للتنبؤ بحالة الهواء عند مغادرة ملف التبريد (المبخر) من حيث درجة حرارة البصلة الجافة ومحتوى الرطوبة. وقد بين النموذج الرياضي للمبخر مطابقة جيدة مع النتائج العملية للبحث.

1. Introduction

The performance of the vapor compression refrigeration system (VCRS) was studied along time ago. However, still too many investigations are to be conducted in order to resolve any problem arises during operation of these systems. Stoecker (1971) [1] developed a thermodynamic cycle computer program to predict the steady state performance of a thermal system. This work produced the performance of the overall system and the influence of each component of the system on its performance. Domanski and Didion (1983) [2] developed a general computer model for the simulation of steady state performance of a split residential air to air heat pump equipped with a capillary tube. This model was verified against three heat pump systems in the cooling mode and one in both cooling and heating modes covering the whole range of heat pump operating conditions. Hamilton and Miller (1990) [3] presented a general steady state model for simulation an air conditioning system. The model depends on the individual component constitutive equation for mass and heat transfer. The work was valuable to air conditioning system original equipment manufacturing since the system design can be generated quickly by specifying various coils, compressor, condenser, capillary tubes and evaporator. Many other investigators dealt with the prediction of thermal design of the refrigeration system such as Hussain (1998) [4] and Thamer (2003) [5]. None of these researches presented the thermal design of the cooling coil in full description from the elementary thermal design point of view.

The present research expresses the following points in a suggested mathematical model:

1. Thermodynamic properties formulation of refrigerant were estimated by Martin and Hou (1995) [6] for R-22 together with thermo physical property formulation established by *ASHRAE* (1997) [7].
2. The ideal and actual coefficient of performance of the system will be predicted depending on the calculation mode developed by the suggested scheme.
3. Thermal design of the cooling coil, evaporator, will be accomplished to predict the conditioned air condition out of the cooling unit including the effect of the presence of humidity with air stream.
4. Taking into account the effect of changing of the environment conditions such as dry bulb temperature and humidity on the above parameters.

2. Experimental Work and Results

The tests were conducted on an available laboratory air cooling unit, as shown in **Fig.(1)**. This unit was suitable for altering the air condition before passing through the cooling coil, evaporator. The dry bulb temperature and moisture content handled by the air may be changed by using the electric heater, **Fig.(1)** and steam diffuser. A schematic diagram of the plate finned tube evaporator of the cooling unit is shown in **Fig.(2)**. The evaporator characteristic basic design, detailed dimensions of its geometry and physical features are listed in **Table (1)**.

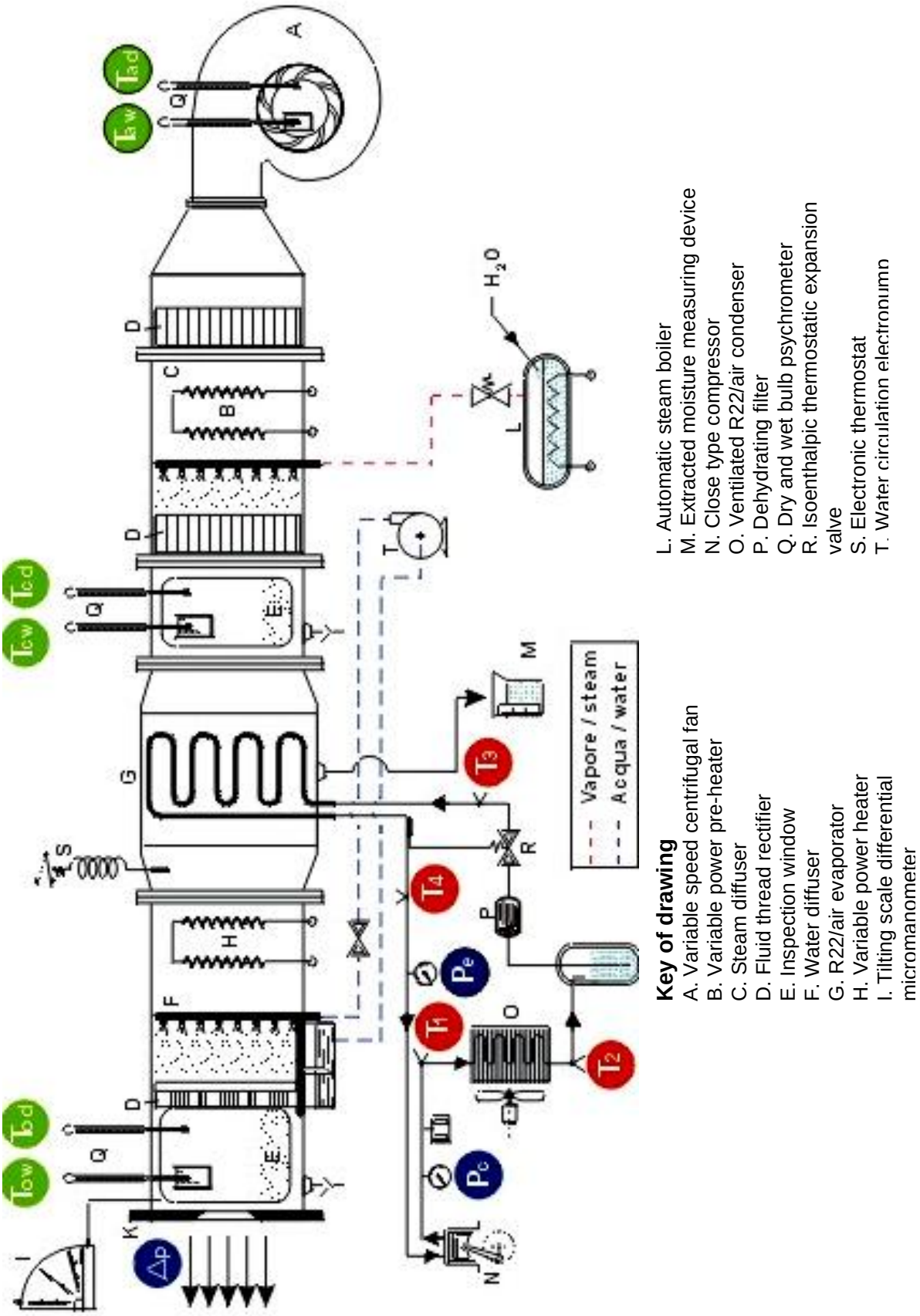

Figure (1) Schematic diagram of the test apparatus

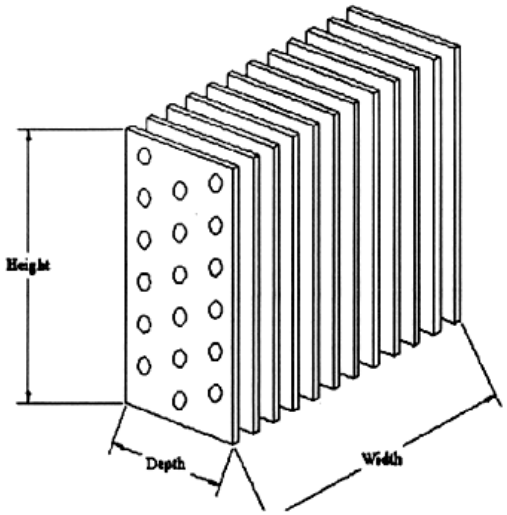

Figure (2a) General heat exchanger dimensions

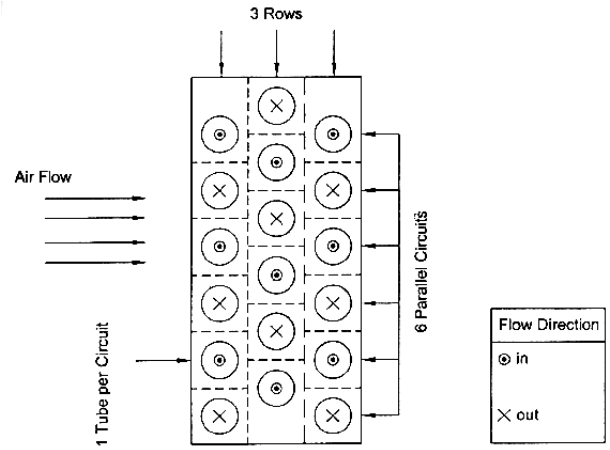

Figure (2b) Layout of heat exchanger geometry parameters

Table (1) Base case evaporator characteristics

Characteristic	Evaporator
Tube spacing in direction parallel to air flow (mm)	15.857
Tube spacing in direction normal to air flow (mm)	25.4
Height of the evaporator (cm)	15.24
Width of the evaporator (cm)	26.5
Depth of the evaporator (cm)	4.776
Number of rows	3
Number of parallel circuits	6
Number of evaporator tubes/circuits	1
Tube inner diameter (mm)	8.865
Tube outer diameter (mm)	9.525
Number of fins/inch (FPI)	8
Fin thickness (mm)	0.1524

The tests were conducted at various conditions of air at the inlet to the cooling coil including dry bulb temperature and humidity contents. The tests may be divided into two categories as follows:

i. Sensible condition only in which the cooling process was performed without adding of moisture to the air stream prior to cooling coil as shown in **Table (2)**.

ii. Humidification and cooling process in which the cooling mode was accomplished by adding of moisture to the air stream before passing through the cooling coil, **Table (2)**.

Table (2) The range of experimental work of the air side of cooling unit

Set Number	Air Mass Flow Rate (kg/hr)	Entering Air Temp. Range (T_{cd}/T_{cw})	Cooling Load (kW)
Sensible (1)	169 - 174	24/14 - 52/24	0.7 - 1.6
Sensible (2)	177 - 180	28/17 - 46/23	0.95 - 1.5
Sensible (3)	169 - 173	33/21 - 58/28	1.0 - 1.75
Sensible (4)	215 - 220	30/18 - 47/24	0.96 - 1.4
Humidification (5)	159 - 162.5	30/18 - 51/28	1.1 - 2.1
Humidification (6)	230 - 235	32/20 - 45/30	1.1 - 1.9
Humidification (7)	205 - 210	34/21 - 53/30	1.0 - 2.1

The above notations refers to the air condition before passing the evaporator and do not describe the cooling process of air as it passes the coil. However, the tests include latent and sensible loads of the air due to the change in its temperature and humidity contents.

Table (3) shows a sample of the experimental data obtained for set no.(1) and set no.(7) conducted at the lower and upper limits of dry bulb and wet bulb temperatures with quite moderate levels of air mass flow rates used during the range of tests. More detailed description of tests conducting procedure is presented by Shehhab (2005) [8].

Table (3a) Experimental data for sensible cooling test at various entering air temperature for set no.(1), see Fig.(1) for refrigerant side condition

Test No.	T_1 (C°)	T_2 (C°)	T_3 (C°)	T_4 (C°)	P_c (bar)	P_e (bar)	T_{ad} (C°)	T_{aw} (C°)	T_{cd} (C°)	T_{cw} (C°)	T_{od} (C°)	T_{ow} (C°)
(1)	54.1	27.7	6.9	10	12.8	4.5	23.9	14.3	23.9	14.3	10.5	8.5
(2)	57.3	28.9	8.1	12.3	13.2	4.66	23.9	14.3	29.8	16.8	15	10
(3)	60.6	30.1	9.1	14.0	13.8	4.8	23.9	14.3	34.7	18.8	18	11
(4)	61.6	31.2	10.6	16.3	14.25	5.1	23.9	14.3	39.9	20.4	22	11.8
(5)	62.8	32.3	12.0	18.1	14.6	5.3	23.9	14.3	46.0	22.5	25.8	12.7
(6)	63.8	33.4	13.7	19.7	14.95	5.66	23.9	14.3	51.8	23.8	29.3	13.5

Table (3b) Experimental data for humidification and cooling process at different dry bulb temperature and specific humidity of air, see Fig.(1) for refrigerant side condition

Test No.	T_1 (C°)	T_2 (C°)	T_3 (C°)	T_4 (C°)	P_c (bar)	P_e (bar)	T_{ad} (C°)	T_{aw} (C°)	T_{cd} (C°)	T_{cw} (C°)	T_{od} (C°)	T_{ow} (C°)
(1)	77.8	46.5	17.7	21.2	18.1	4.7	34	21	34	21	19	15.5
(2)	80	49.1	19.6	22.7	18.7	4.9	34	21	37.6	23.1	22	16.6
(3)	84.1	51.2	20	24.3	19.1	5.1	34	21	41.1	25.2	25	18
(4)	86.3	53.2	22.1	27.2	19.7	5.3	34	21	44.6	27	27.9	19.6
(5)	88.1	56.8	25.4	30.1	20.4	5.5	34	21	49	28.7	32	21
(6)	90.2	58.5	28.3	33.4	20.9	5.8	34	21	53.1	30.4	33.8	22.2

3. Theoretical Assessment

3.1 Refrigerant Side

A standard vapor compression refrigeration cycle is shown in **Fig.(3)** on the (p-h) diagram. The refrigeration load of the cycle is estimated by:

$$Q_{evap} = m_r(h_4 - h_3) + m_r cp_g(T_4 - T_{\bar{4}}) \quad \text{..... (1)}$$

And the condensing load of the condenser is represented as:

$$Q_{cond} = m_r(h_1 - h_{\bar{2}}) + m_r cp_{\ell}(T_{\bar{2}} - T_2) \quad \text{..... (2)}$$

For such cycle, the compressor work is written as:

$$W_{comp} = m_r(h_1 - h_4) \quad \text{..... (3)}$$

The above equation gives the performance index defined as coefficient of performance (COP) in the form:

$$COP = \frac{(h_4 - h_3)}{(h_1 - h_4)} \quad \text{..... (4)}$$

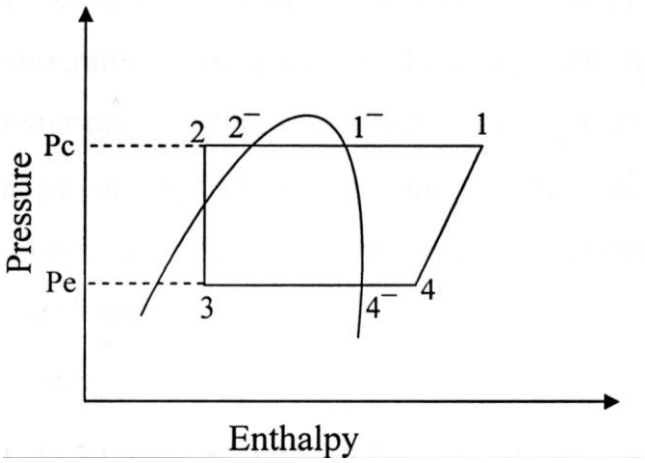

Figure (3) Standard vapor compression refrigeration cycle (p-h) diagram

3.2 Air Side

The total heat removed from the air stream passing through the cooling coil, evaporator, is estimated by:

$$Q_{evap} = m_a (h_{exit} - h_{inlet})_{evap} \quad \text{..... (5)}$$

The air enthalpy depends on the air condition, dry bulb temperature and wet bulb temperature at the considered position with respect to the evaporator. The sensible load removed from air is estimated from:

$$Q_{sen} = m_a cp_{Hum} (T_{exit} - T_{inlet})_{evap} \quad \text{..... (6a)}$$

The humid heat of the humidified air consists of two components of the dry air specific heat and the vapor specific heat in the form:

$$cp_{Hum} = cp_a + cp_g w \quad \text{..... (6b)}$$

Its value is in the range between (1.013) and (1.026) for most of the air conditioning practical applications.

And the latent load part from:

$$Q_{lat} = m_a (w_{inlet} - w_{exit}) 2501 \quad \text{..... (6c)}$$

The summation of the individual parts of cooling load, eq.(6) will produce the evaporator load (Q_{evap}) as well.

Some considerations must be made for the dehumidification process taking place on the cooling coil surface as the moist air passes. The specific heat of air is corrected to account for condensation. Because the air flowing over the evaporator is cooled below the dew bulb temperature, some of the heat is rejected by the air results in condensing water out of the air

rather than lowering the temperature, as shown in **Fig.(3)**. The total enthalpy change of the air is represented by:

$$\Delta h_{tot} = \Delta h_{sen} + \Delta h_{lat} \quad \text{..... (7a)}$$

$$\frac{\Delta h_{tot}}{\Delta T} = \frac{\Delta h_{sen}}{\Delta T} + \frac{\Delta h_{lat}}{\Delta T} \quad \text{..... (7b)}$$

$$cp_{eff} = cp_{Hum} + \frac{\Delta h_{lat}}{\Delta T} \quad \text{..... (7c)}$$

Salder (2000) [9] showed experimentally that the latent enthalpy accounts for about 25% of the total enthalpy change for air flowing over an evaporator in residential applications. Therefore, the following form may be deduced for the effective air enthalpy

$$cp_{eff} = 1.33 cp_{Hum} \quad \text{..... (8)}$$

This expression will be used whenever it is suitable for cooling coil performance prediction in this research.

4. Evaporator Performance Prediction

The analysis of the evaporator designed will depend on the actual process takes place on both refrigerant and air sides. On the refrigerant side, two zones may be observed; they are the saturation vaporization and superheating stages, as shown in **Fig.(4)**. These processes are accomplished by changing of the air conditions it passes through the cooling coil.

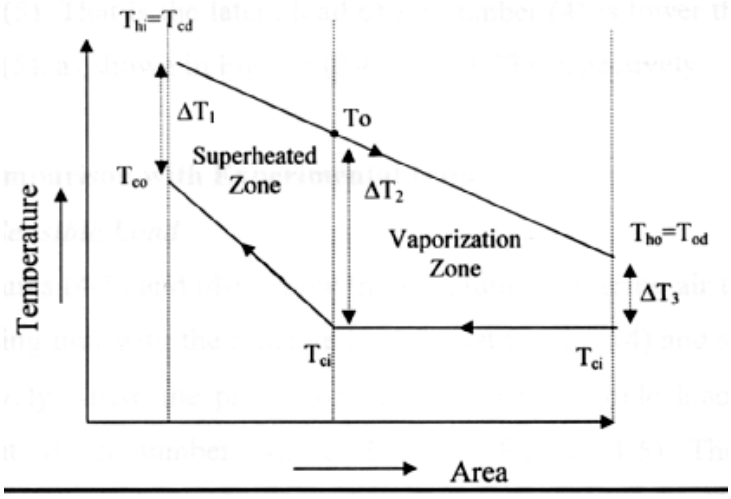

Figure (4) Thermal diagram for general case of coil surface operates partially dry

4.1 Refrigerant Side Heat Transfer Coefficient

The heat transfer coefficient between the refrigerant and tube wall in the two phase flow region in evaporator is obtained with a compilation of theories and experiments, using the Lockart-Martinelli parameter (1949) [10]. The correlation of the local heat transfer coefficient is:

$$\bar{h}_r = C\left(\frac{1}{Xu}\right)^n h_\ell \quad \text{..... (9a)}$$

where, the single phase heat transfer coefficient is estimated from:

$$h_\ell = 0.023\left(\frac{k_\ell}{d}\right)(Re_\ell)^{0.8}(Pr_\ell)^{0.4} \quad \text{..... (9b)}$$

$$Xu = \left(\frac{\mu_\ell}{\mu_\upsilon}\right)^{0.1}\left(\frac{\rho_\upsilon}{\rho_\ell}\right)^{0.5}\left(\frac{1-x}{x}\right)^{0.9} \quad \text{..... (9c)}$$

$$Re_\ell = \frac{4m_r}{\pi d_i \mu_\ell} \quad \text{..... (9d)}$$

$$Pr_\ell = \frac{cp_\ell \mu_\ell}{k_\ell} \quad \text{..... (9e)}$$

The constants (C) and (n) depend on operation conditions. In horizontal pies, with commonly used refrigerants [10] where for turbulent flow C=3.5 and n=0.45.

In the superheating zone, the equation for single phase flow heat transfer coefficient is the Dittus-Boelter (1973) [11], eq.(9.b) may be used with using the vapor properties and parameters.

4.2 Air Side Heat Transfer Coefficient

The work of McQuiston (1988) [12], was used with some modification to evaluate the air side convective heat transfer coefficient for plate fin heat exchanger with multiple rows of staggered tubes, as shown in **Fig.(2)**. The heat transfer coefficient is based on the Colburn j-factor which is defined as:

$$j = St(Pr)^{2/3}$$

Which gives:

$$\bar{h}_a = \frac{jcp_a G_{max}}{(Pr)^{2/3}} \quad \text{..... (10)}$$

where: $G_{max} = \dfrac{m_a}{A_{min}}$

and the minimum flow area as:

$$A_{min} = \omega(1 - FPt)(H - tpcN_c d_o)$$

McQuiston found that the j-factor for four row finned tube heat exchanger fits a linear model based on the parameter (JP), where:

$$j_4 = 0.2675JP + 1.325E - 06 \quad \text{..... (11a)}$$

$$JP = (Re_d)^{-0.4}\left(\frac{A_o}{A_t}\right)^{-0.15} \quad \text{..... (11b)}$$

In which the Reynolds number is based on the outside diameter of the tube, d_o, and the maximum mass velocity G_{max}. The heat transfer coefficient for heat exchanger with four or less rows can be found using the following correlation:

$$\frac{j_n}{j_4} = \frac{1 - (1280)(n)(Re_L)_a^{-1.2}}{1 - (1280)(4)(Re_L)_a^{-1.2}} \quad \text{..... (12)}$$

$(Re_L)_a$ is based on the row horizontal spacing X_L

$$(Re_L)_a = \frac{G_{max} X_L}{\mu_a}$$

The modification suggested in this work concerns the moist air properties especially, the specific heat of the humid air used in eq.(10), Shehhab [8]. The idea of eq.(7c) is applied whenever it is required for the prediction of the moist air side heat transfer coefficient for the thermal design of the evaporator. This suggestion is incorporated in a computer program built for this purpose in this investigation.

4.3 Overall Heat Transfer Coefficient

The overall heat transfer coefficient, U, neglecting the wall resistance and the fouling resistance on both sides of the heat exchanger, may be estimated from the following

$$UA = \left[\frac{1}{\eta_s \bar{h}_a A_a} + \frac{1}{\bar{h}_r A_r}\right]^{-1} \quad \text{..... (13a)}$$

where:

$$\frac{1}{UA} = \frac{1}{U_r A_r} = \frac{1}{U_a A_a}$$

$$\eta_s = 1 - \frac{A_f}{A_o}(1 - \eta_f) \quad \text{..... (13b)}$$

$$\eta_f = \frac{\tanh(mr_e\phi')}{(mr_e\phi')} \quad \text{..... (13c)}$$

McQuiston [12] analyzed hexagonal fins and show that, they could be treated like circular fins by replacing the outer radius of the fin with an equivalent radius

$$\frac{r_e}{r} = 1.27\psi(\beta - 0.3)^{1/2}$$

The coefficients ψ and β are defined as:

$$\psi = \frac{X_T}{2r} \quad \text{..... (14a)}$$

$$\beta = \frac{1}{X_T}[X_L{}^2 + \frac{X_T{}^2}{4}]^{1/2} \quad \text{..... (14b)}$$

The parameter (m) may be calculated from:

$$m = (\frac{2\bar{h}_a}{kt}) \quad \text{..... (14c)}$$

And for circular tubes, the parameter ϕ' is defined as:

$$\phi' = [\frac{r_e}{r} - 1][1 + 0.35\ln(\frac{r_e}{r})] \quad \text{..... (14d)}$$

4.4 Air Exit Dry Bulb Temperature Estimation

The theoretical part concerning the evaporator thermal design is based on the prediction of the exit air temperature and humidity for any specified entering air condition. Referring to **Fig.(4)**, the total heat rejected from the hot fluid (air) in the superheating zone can be estimated by:

$$Q_{sup} = m_r(h_4 - h_{\bar{4}}) \quad \text{..... (15)}$$

In this region, the air side exit dry bulb temperature leaving the cooling coil is (T_o) and may be calculated from:

$$T_o = T_{cd} - \frac{Q_{sup}}{m_a cp_{Hum}} \quad \text{..... (16)}$$

where: (T_{cd}) is the inlet air dry bulb temperature to the evaporator. The outlet temperature (T_o) from the superheating zone is considered to be as the inlet air temperature to the vaporization

zone. The total heat rejected from this zone is (Q_{evap}) and can be calculated from the following equation:

$$Q_{evap} = m_r (h_{\bar{4}} - h_3) \quad \text{..... (17)}$$

And the exit air temperature from the vaporization zone is estimated by:

$$T_{od} = T_o - \frac{Q_{evap}}{m_a cp_{Hum}} \quad \text{..... (18)}$$

where, (T_{od}) represents the outlet air dry bulb temperature from the cooling coil, evaporator.

The area required for each portion, superheating and vaporization was calculated in a numerical technique including iteration procedure for which energy balance and mass balance of vapor content was proved. This procedure was incorporated in the computer program built for this purpose.

5. Results and Discussion

For this purpose, the results of the experimental work of set number (4) and (5) are used for the performance prediction. These sets are chosen to show the capability of the theoretical model presented in this work in response to the effect of the presence of humidity on its prediction. That is the moisture content of air of set no.(4) is lower that that of set no.(5). In other words, the latent load of set no.(4) is lower than that of set no.(5).

5.1 Sensible Load

A comparison between the experimental and theoretical prediction of sensible load portion is shown in **Figs.(5a)** and **(5b)** for sets no.(4) and (5) respectively. The results showed that the comparison has the same trend for both experimental and theoretical values. The discrepancy between these values is varied between (0.06 and 0.14 kW) for the whole range of the tested air inlet temperature of set no.(4), **Fig.(5a)**. While, the corresponding deviations percentage between the predicted and measured data are (5%) and (12%) for the whole range of test temperature of set no.(5), **Fig.(5b)**. The deviation percentage is defined as:

$$\varepsilon\% = \frac{Predicted - Actual}{Predicted} \times 100 \quad \text{..... (19)}$$

And the discrepancy is defined as the absolute difference between any two variables at the same conditions. These curves of **Fig.(5)** show that increasing of the inlet air dry bulb temperature to the cooling coil exhibits an improvement to the sensible load due to the increasing value of the potential temperature difference across the cooling coil of the unit.

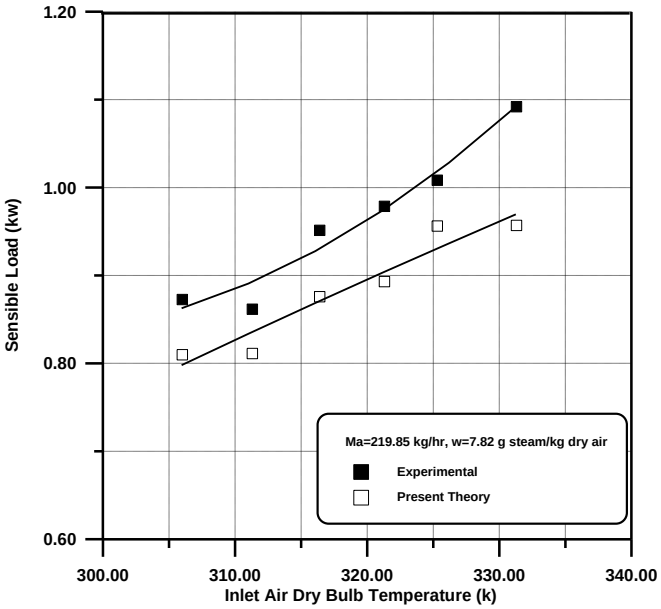

(a) Sensible cooling test

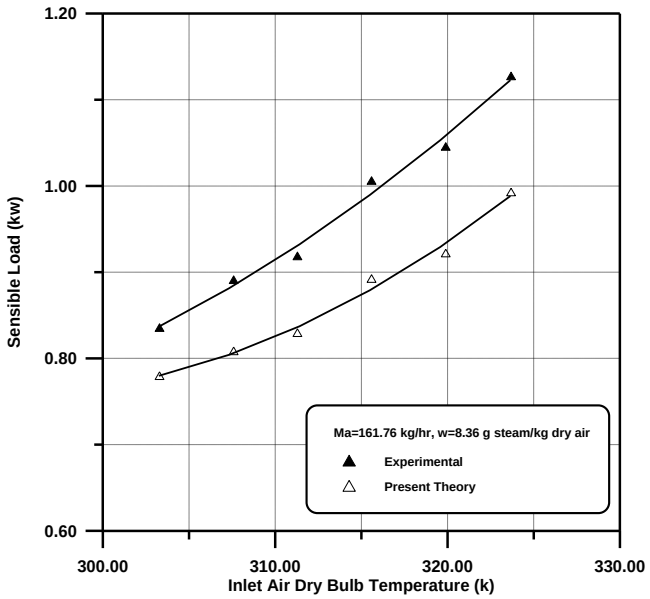

(b) Humidification cooling test

Figure (5) Comparison between experimental sensible load with the predicted value of the present model

5.2 Latent Load

The results of the experimental data and theoretical values are shown in **Fig.(6)**. The maximum error in the load estimation for set no.(4) occurs at inlet air temperature of (331 K) corresponds to (0.05 kW). The deviation value for set no.(5) occurs at (324 K) and corresponds to a value of (0.14 kW). The latent load represents the rate of vapor condensation out of the air stream which depends on the cooling criteria of the air to a temperature below its original dew point. Further, condensation takes places whenever the air stream comes into contact with a cold surface at a temperature below of its entering dew temperature. The cooling coil showed a capability of increasing the rate of condensation, latent load, as the

humidity content of air was increased, as shown in **Fig.(6)**. The trend of the experimental and theoretical data concluded that a maximum latent load can be approached, where any increase of the humidity contents will not produce any increase of the latent load due to the limitation capacity of the cooling coil. That is for any specified design of the cooling unit, there is an optimum value for the condensation rate which can be withdrawn out of the air stream passing the cooling coil for a given condition.

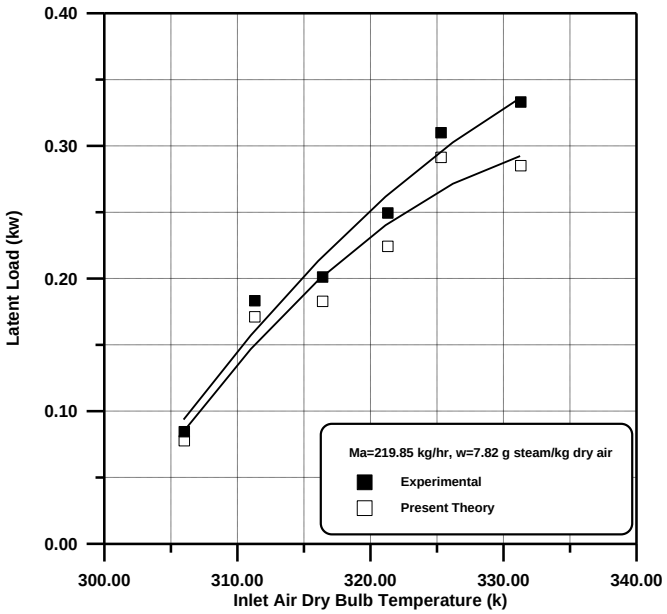

(a) Sensible cooling test

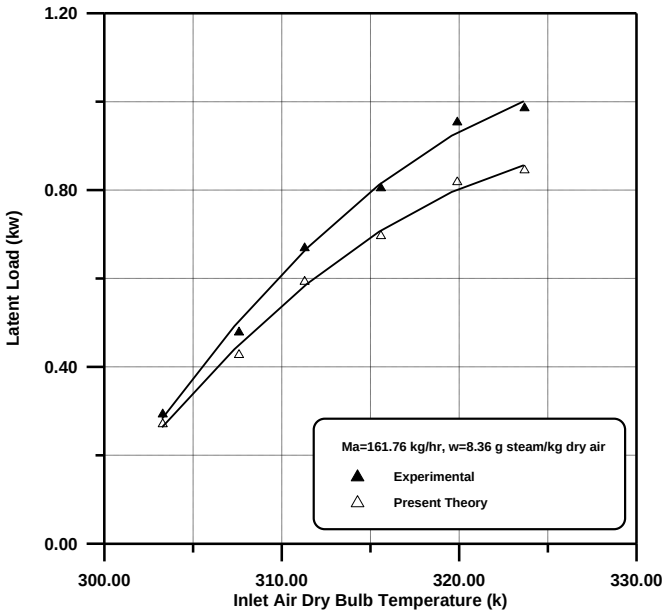

(b) Humidification cooling test

Figure (6) Comparison between experimental latent load with the predicted value of the present model

5.3 Total Refrigeration Load

The total refrigeration load of the above sets predicted by the model is compared to the actual data in **Fig.(7)**. Again, the results showed that the predicted values are very close at low entering air temperature compared with a difference at (306 K) and (303 K) for sets (4) and (5) corresponding to (0.07 kW) and (0.08 kW) respectively. These values increase to (0.18 kW) and (0.28 kW) at (331 K) and (324 K) for sets (4) and (5) respectively. It is obvious that the trend of the curves of both of the model and tests is the same. This behavior shows that increasing of the entering air dry bulb temperature reveals an increase of the total cooling load of the refrigeration system. This of course is due to the increase of both sensible and latent loads as described above. For comparison, the experimental data showed that the total load of set no.(5) was higher than that of set no.(4) for entering air temperatures of (305 K) and (320 K) by (21 %) and (35 %) respectively.

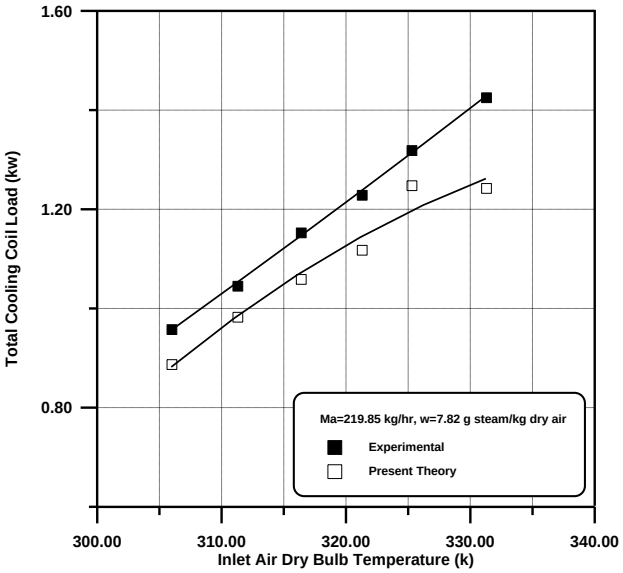

(a) Sensible cooling test

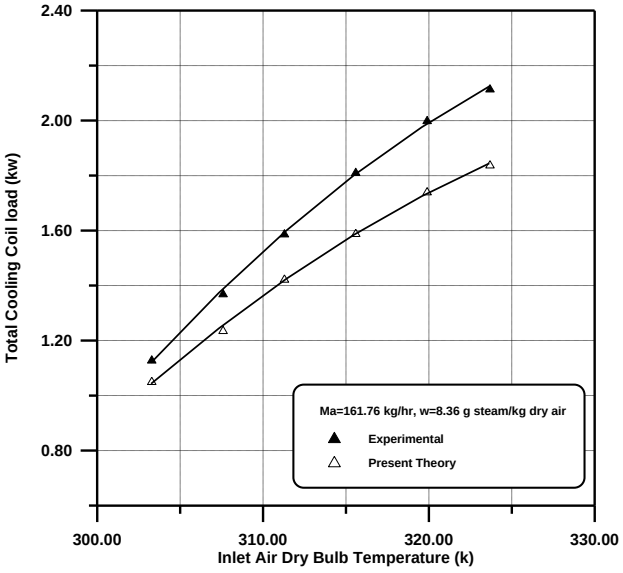

(b) Humidification cooling test

Figure (7) Comparison between experimental total load with the predicted value of the present model

5.4 Compressor Work

The compressor work (actual, estimated and ideal) for the above sets is shown in **Fig.(8)**. The actual and estimated values for set no.(4) show a slight difference for the range of temperature between (306 K) and (331 K), although they show almost the same trend. The ideal work reveals lower values of compressor work than those of actual and estimated values.

For set no.(5), the results show a smooth behavior of all curves for actual, estimated and ideal compressor work. The discrepancy between the estimated and actual values ranges between (0.08 hp) and (0.23 hp) for temperature ranges between (303 K) and (324 K) respectively. Again, the ideal values are lower than those of the actual and predicted work, its value ranges between (0.2 hp) and (0.35 hp) for the whole range of temperature tested between (303 K) to (324 K) respectively. On the other hand, the corresponding values of the estimated and actual work are (0.3-0.7 hp) and (0.2-0.5 hp) respectively.

When both results of set no.(5) and set no.(4) are compared at an inlet air dry bulb temperatures of (305 K) and (320 K), the compressor work of set no.(5) was higher than those of set no.(4) by (46 %) and (60 %) respectively. This of course was because of the higher cooling load of set no.(5) than that of set no.(4). The curves showed that increasing the entering air temperature causes an increase of the compressor work was due to cooling load increase.

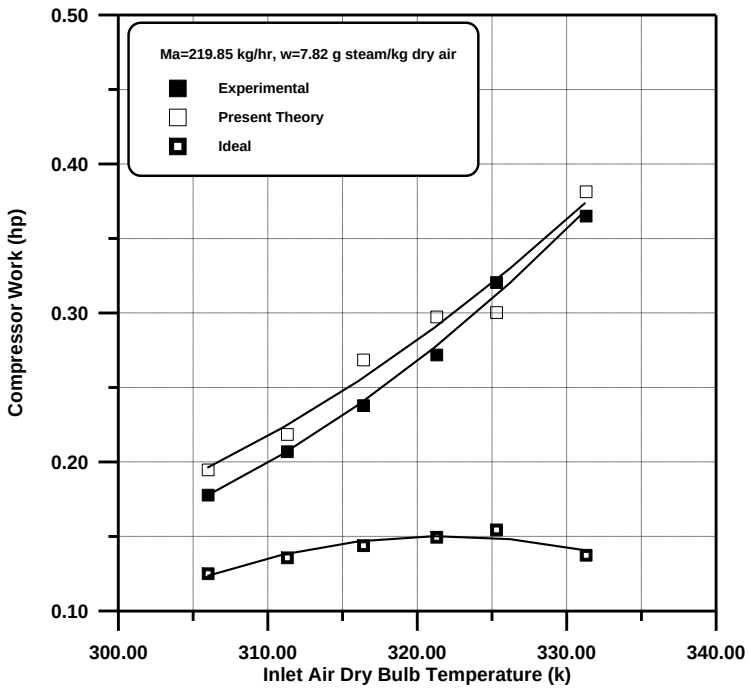

(a) Sensible cooling test

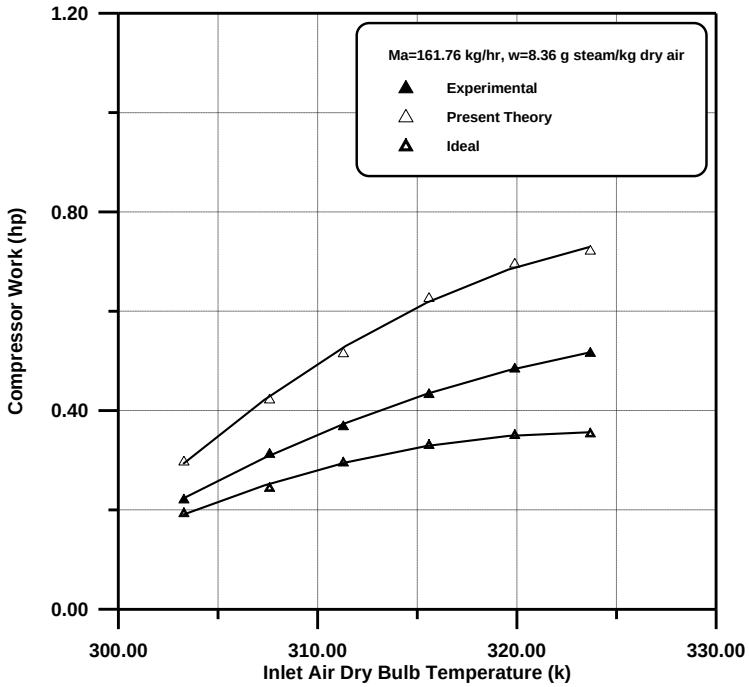

(b) Humidification cooling test

Figure (8) Comparison between experimental and predicted work of compressor with the value of the present model

5.5 Coefficient of Performance (COP)

Figure (9) shows the actual, estimated and ideal coefficient of performance for sets (4) and (5). The actual and estimated values for set no.(4) showed a slight difference for the temperature ranging between (306 K) and (331 K) although they show almost the same trend. The difference between actual and estimated values when compared with the ideal value shows a discrepancy ranging between (3.5) and (9.3) for the above temperature range.

For set no.(5), the (COP) curves of all of types, actual, estimated and ideal show smooth behavior. The discrepancy between the estimated and the actual values ranges between (0.5) and (0.7) for the temperature ranging between (303 K) and (324 K) respectively. Again, the ideal (COP) values which are higher than those of the actual and predicted coefficient of performance was about (7) for the whole range of air inlet temperature to the cooling coil. On the other hand, the corresponding values of the estimated and the actual (COP) are (6.3-4.8) and (6.8-5.5) respectively.

The results of set no.(5) and set no.(4) showed that increasing of the entering air temperature to the cooling coil led to a reduction in the coefficient of performance in spite of the total cooling load increase. This was as a result to the fact that although the compressor was increased as the load increased, but it has a percentage rate higher than that of load increase. Both sets exhibited almost equal (COP) range between (7) and (5.5) for the cooling unit for temperatures of (305 K) and (325 K) respectively.

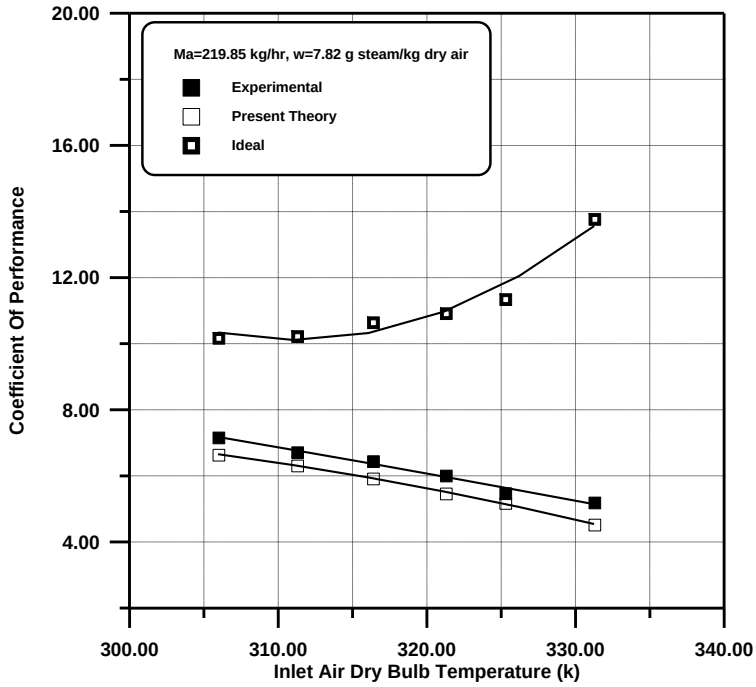

(a) Sensible cooling test

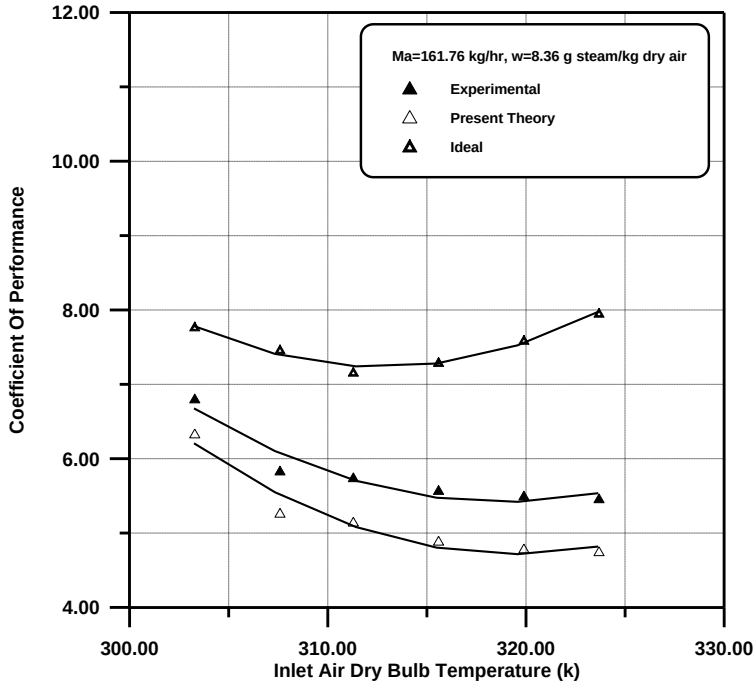

(b) Humidification cooling test

Figure (9) Comparison between experimental and predicted (COP) with the ideal value of the present model

6. Conclusion

The findings which can be withdrawn from this study can be summarized as follows:

- The experiments conducted in this study showed the rapid response of the cooling unit performance to any variation of the environment conditions. Increasing of the entering air dry bulb temperature and humidity contents produces an increase of the total load and compressor work of the cooling unit by different proportional. For a given air temperature, the coefficient of performance (COP) was not affected greatly by the humidity content variation. But for a given air condition, temperature and humidity content, the (COP) showed a reduction with increasing of the entering air temperature. For a specified thermal and mechanical design of an air conditioning system, there is a limit for the cooling capacity, sensible and latent, where could not be overcome.
- The theoretical model and computer program built for this study showed a high reliability in application for the prediction of the exit air condition as the evaporator entering air condition, temperature and humidity content varies. The predicted values of cooling load, compressor work and coefficient of performance agreed well with the experimental data.

7. References

1. Stoecker, W. F., ***"A Generalized Program for Steady State System Simulation"***, ASHRAE Trans., Vol. 77, 1971, pp. 140-148.

2. Domanski, P., and Didion, D., ***"Computer Modeling of the Vapor Compression Cycle With Constant Flow Area of Expansion Device"***, Building Science 155, National Bureau of Standards, Washington DC., USA, 1983.

3. Hamilton, J. F., and Miller, J. L., ***"A Simulation Program for Modeling Air Conditioning System"***, ASHRAE Trans., Vol. 96, Part (1), 1990, pp. 213-221.

4. Hussain, R. M., ***"A Numerical Simulation of Vapor Compression Refrigeration Cycle Using Alternative Refrigerants"***, Ph.D. Thesis, Mech. Eng. Dept., Baghdad University, 1998.

5. Thamer, K. S., ***"Air to Air Refrigeration Cycle Compared With Conventional Refrigeration in Air Craft"***, M.Sc. Thesis, Mech. Eng. Dept., University of Al-Rasheed, 2003.

6. Martine, J. J., and Hou, Y. C., ***"Development of a New Equation of State for Gases"***, AIchE. Journal, Vol. (1), 1955, pp. 142-154.

7. ***"Thermodynamic Properties of Refrigerants"***, ASHRAE, 1997.

8. Shehhab, U. S., ***"Theoretical and Experimental Studies of Environment Effect on the Performance of Air Conditioning System"***, M.Sc. Thesis, Mechanical Engineering Department, Al-Mustansiriya University, 2005.

9. Salder, E. M., ***"Design Analysis of a Finned Tube Condenser for a Residential Air Conditioner Using R-22"***, M.Sc. Thesis, Mech. Eng. Dept., Georgia Institute of Technology, April, 2000.

10. Lockhart, R. W., and Martinelli, R. C., ***"Chemical Engineering Progress"***, Vol. 45, 1949, 39 pp.

11. Dittus, F. W., and Boelter, L. M. K., ***"Correlation on Flow Resistance and Heat Transfer"***, Trans. of ASME, Vol. 59, 1973, pp. 583-594.

12. McQuiston, F. C., ***"Heating Ventilating and Air Conditioning"***, Analysis and Design, 3rd Edition, 1988.

Nomenclature

A:	Surface Area (m^2)
A_{min}:	Minimum Flow Area (m^2)
C:	Constant Defined in eq.(9.a)
cp:	Specific Heat (kJ/kg.K)
cp_{eff}:	Effective Specific Heat (kJ/kg.K)
cp_{Hum}:	Humid Heat (kJ/kg.K)
FP:	Fin Pitch (m)
G:	Mass Velocity (kg/m^2 s)
h:	Enthalpy (kJ/kg)
$\bar{h}$:	Heat Transfer Coefficient (W/m^2 K)
H:	Heat Exchanger Height (m)
m:	Mass Flow rate (kg/s) or Constant
N_c:	Number of Parallel Circuits
Pr:	Prandtle Number (Dimensionless)
Q_{evap}:	Evaporator Capacity (kW)
Q_{cond}:	Condenser Heat Rejected (kW)
r:	Outside Tube Radius (m)
r_e:	Equivalent Radius (m)
Re:	Reynolds Number (Dimensionless)
St:	Stanton Number (Dimensionless)
t:	Fin Thickness (m)
T:	Temperature (C°)
tpc:	Tubes per Circuit (Dimensionless)
U:	Overall Heat Transfer Coefficient (W/m^2 K)
w:	Specific Humidity of Air (kg. steam/kg d.a.)
W_{comp}:	Compressor Work (kW)
x:	Quality (Dimensionless)
X_L:	Longitudinal Tube Spacing (Parallel to Air Flow), (m)

X_T: Transverse Tube Spacing Normal to Flow, (m)
Xu: Lochart-Martinelli Parameter (Dimensionless)
Δh: Enthalpy Change (kJ/kg)

Greek Symbols

ε: Deviation Percentage (Dimensionless)
ϕ': Fin Parameter Defined by eq.(14.d), (Dimensionless)
β: Fin Parameter Defined by eq.(14.b), (Dimensionless)
μ: Dynamic Viscosity (kg/m.s)
ω: Heat Exchanger Width (m)
ρ: Density (kg/m^3)
η_f: Fin Efficiency Defined by eq.(13.c), (Dimensionless)
η_s: Surface Efficiency Defined by eq.(13.b), (Dimensionless)
ψ: Fin Parameter Defined by eq.(14.a), (Dimensionless)

Subscript

a: Air
comp: Compressor
cond: Condenser
d: Dry Bulb
e: Entering or Equivalent
eff: Effective
evap: Evaporator
g: gas or Vapor
i: Inside or Inlet
ℓ: Liquid
lat: Latent
max: Maximum
min: Minimum
o: Outside
r: Refrigerant
sen: Sensible
sup: Superheating
tot: Total
w: Wet Bulb